Amphibians' expansion to record elevations influences chytrid (*Batrachochytrium dendrobatidis*) infection dynamics

Emma Steigerwald[1, 2,*], Cassandra Gendron[3], Juan C. Chaparro[4], Rosemary G. Gillespie[2], Allie Byrne[1, 2], Rasmus Nielsen[5, 6, 7], Bree Rosenblum[1, 2]

[1] The Museum of Vertebrate Zoology, The University of California at Berkeley, CA, 94720, USA
[2] The Department of Environmental Science, Policy, and Management, The University of California at Berkeley, CA, 94720, USA
[3] The Department of Plant and Microbial Biology, The University of California at Berkeley, CA, 94720, USA
[4] El Museo de Biodiversidad del Perú, Cusco, Perú
[5] The Department of Integrative Biology, The University of California at Berkeley at Berkeley, CA, 94720, USA
[6] The Department of Statistics, The University of California at Berkeley at Berkeley, CA, 94720, USA
[7] The Globe Institute, The University of Copenhagen, 1350, København K, Denmark

*corresponding author. Email: emma.c.steigerwald@gmail.com

ABSTRACT

The climate-driven range shifts of host species could potentially impact emerging infectious disease (EID) events through several mechanisms, with repercussions for conservation and public health. Host range expansion could affect infection outcomes if hosts and pathogens respond differentially to new environments or create novel transmission opportunities if new contact is established between alternate competent host species or populations. Here, we study Marbled four-eyed frogs (*Pleurodema marmoratum*) and their fungal pathogen *Batrachochytrium dendrobatidis* (*Bd*) in the Cordillera Vilcanota, Peru. There, these frogs were recorded as having expanded hundreds of vertical meters into deglaciating habitats to become the highest-living amphibians globally. With field surveys, we establish that range expansion created new opportunities for *Bd* transmission: *P. marmoratum* is now continuously distributed along passages between populations otherwise separated by heavily-glaciated mountains. We sequence Vilcanota *Bd*, finding that it belongs to the lineage most frequently associated with amphibian declines (*Bd*GPL) and characterizing it as lacking genetic structure despite possessing abundant variation, consistent with extensive *Bd* dispersal. Collecting temperature data from *P. marmoratum* microhabitats, we demonstrate that upslope expansion clearly exposed frogs and their pathogen to new thermal regimes. Finally, we analyze field and infection data from individual frogs, concluding that the new elevations colonized by *P. marmoratum* appear to moderately constrain *Bd* infection intensities and influence the sublethal costs of infection: infected frogs at high elevation do not have depressed body conditions like their low-elevation counterparts, but also do not achieve the larger body sizes that uninfected individuals typically reach at higher elevations.

KEYWORDS:

disease triangle —range expansion—transmission — sublethal effects — synergisms — climate change— Cordillera Vilcanota, Peru

INTRODUCTION

The rising incidence of emerging infectious diseases (EIDs) is a critical issue for conservation, public health, and agriculture (Fisher *et al.* 2012; Jones *et al.* 2008). Climate change may contribute to outbreaks through several mechanisms. One of these mechanisms, climate-driven range shifts, is expected to influence the infection dynamics of many important pathogens (Harvell *et al.* 2002; Hoberg & Brooks 2015; Liang & Gong 2017). For example, the upslope expansion of mosquitos in Hawaii is predicted to drive the continued decline of endemic birds currently evading avian malaria at high elevations (Zamora-Vilchis *et al.* 2012). Meanwhile, the northwards expansion of ticks in Europe is predicted to extend the incidence of Lyme infections (Jaenson & Lindgren 2011). Existing data on the interaction of climate-driven range shifts and EIDs largely comes from vector-borne systems, as many vectors are highly sensitive to climate (Harvell *et al.* 2002). However, the widespread climate-driven range shifts of potential host species (Freeman *et al.* 2018; Moritz *et al.* 2008; Parmesan *et al.* 1999) will also likely affect the infection dynamics of non-vector-borne pathogens. As host distributions change, their altered movement patterns and exposure to novel environments could introduce hosts to new pathogens, reshape transmission patterns, or exacerbate or mitigate existing infections.

Several proposed mechanisms link climate change to the emergence of *Batrachochytrium dendrobatidis* (*Bd*; Li *et al.* 2013), a pathogen contributing to devastating global amphibian declines through the disease chytridiomycosis (Scheele *et al.* 2019; Skerratt *et al.* 2007). In some areas, the impact of climate change on local climate may be spatially and/or temporally expanding optimal *Bd* growth conditions (Bosch *et al.* 2007). Meanwhile, more frequent droughts compromise amphibian immunity and enhance *Bd* transmission when amphibians aggregate in wet or humid microhabitats (Burrowes *et al.* 2004; Lampo *et al.* 2006). Higher short-term climatic variability may also disadvantage amphibians relative to *Bd*, as pathogens tend to adapt more rapidly than their hosts under changing conditions (Raffel *et al.* 2013; Rohr & Raffel, 2010). Finally, as parasites generally have broader thermal tolerances than hosts, frogs are more likely to be exposed to suboptimal temperatures than *Bd*, again placing them at a disadvantage (Cohen *et al.* 2019; Cohen *et al.* 2017). Amidst mounting evidence that amphibians are undergoing climate-driven range shifts (e.g. Bustamante *et al.* 2005; Enriquez-Urzelai *et al.* 2019; Raxworthy *et al.* 2008), we aim to explore whether new host movement opportunities and exposure to novel environments provided by these range shifts could influence *Bd* transmission, infection intensities, and sublethal impacts.

The Cordillera Vilcanota, Peru, is an ideal system for exploring how climate-driven range shifts impact EIDs. Surveys of this heavily glaciated tropical mountain chain in the 2000s revealed that the Marbled four-eyed frog (*Pleurodema marmoratum*) had expanded its upper range limit by hundreds of vertical meters within the mountain pass "Osjollo" to a record elevation of 5,400 m asl, making it the highest elevation amphibian globally (Seimon *et al.* 2007). The timeline for the upslope expansion of *P. marmoratum* is constrained by the contemporary deglaciation of Osjollo

Pass, which began during the Little Ice Age but continued until at least 1980, when the last ice-bound portions of Osjollo Pass melted open (Seimon *et al.* 2017). Early amphibian surveys of the Vilcanota also documented the first known *Bd* infections and *Bd*-induced amphibian die-offs in southern Peru (Seimon *et al.* 2005; Seimon *et al.* 2007). *P. marmoratum* was found to be susceptible to chytridiomycosis, the disease caused by *Bd,* and *P. marmoratum* with symptomatic chytridiomycosis continued to be documented until the most recent field surveys in 2015 (Seimon *et al.* 2017).

Here, we explore the repercussions of the elevational range expansion of *P. marmoratum* on the transmission, intensity, and sublethal costs of *Bd* infections. We hypothesized that

I. We will find that *P. marmoratum* are now continuously distributed across the deglaciated passage provided by Osjollo Pass. This new contact between frog populations separated by the heavily glaciated Cordillera Vilcanota would provide new routes for direct *Bd* transmission.
II. We will find that both *P. marmoratum* and *Bd* will be increasingly exposed to challenging thermal conditions as elevation increases. Amphibians will be increasingly exposed to the limits of their thermal tolerance and *Bd* will have narrower daily windows for replication.
III. We will find Vilcanota *Bd* to belong to the lineage most associated with *Bd* epizootics in South America, the Global Panzootic Lineage (Farrer *et al.* 2011).
IV. While we expect changing frog distributions to create new routes for *Bd* transmission between populations (hypothesis I), local conditions (dry, cold) at the highest elevations inhabited by amphibians globally will hamper the dispersal of *Bd* in the Vilcanota such that it will be genetically structured by watersheds, as observed at high elevations in California (Rothstein *et al.* 2021). This spatial structure would contrast with most places where *Bd* has been sequenced, where *Bd* disperses easily so lacks structure (Alvarado-Rybak *et al.* 2021; Basanta *et al.* 2021; Byrne *et al.* 2019).
V. The new elevations frogs have colonized contrain *Bd* infection intensities, given that we expect increasing elevations to limit opportunities for *Bd* replication temporally (hypothesis II). The present study, which includes data beyond 5,300 m asl, is the first to examine *Bd* infection intensities above 4,000 m asl, but previous studies have suggested that the prevalence of *Bd* infections may be limited possibly even before 4000 m asl, perhaps by increasingly unsuitable thermal conditions for *Bd* replication (Catenazzi *et al.* 2011; Muths *et al.* 2008).
VI. *Bd* infection has different sublethal costs for *P. marmoratum* across elevations. Potentially, amphibians living closer to their physiological limits at 5,400 m asl (hypothesis V) will be more impacted by infection and have smaller body conditions and sizes. Alternately, *Bd* replication at 5,400 m asl could be limited (hypothesis V) to the extent that frogs will have higher body conditions and sizes.

METHODS

1. Field sampling

We sampled *P. marmoratum* in the Cordillera Vilcanota, a mountain chain in the Peruvian Andes, during their final breeding months (March-May) in 2018 and 2019. Sampling sites

ranged from 3,967—5,333 m asl (Figure 1; contour map in Figure S 1), and were spaced 5—10 km apart in a circuit around the base of the mountains and 1—3 km apart across two mountain passes—lower points between peaks that can provide a route for passage across mountains. The western pass, Osjollo, measures approximately 13 km across and was blocked by glacial ice until after 1980 (Figure 1; Seimon et al. 2007). We searched for tadpoles in ponds and bogs, and for post-metamorphic stages under rocks. We attempted to capture 15 adults per site, supplementing first with juveniles and then with tadpoles. Life stage was recorded as adult (310 individuals), juvenile (74 individuals), or as a Gosner developmental stage (232 individuals; Gosner 1960). We noted snout-vent length (SVL, in mm), mass (in g), and signs of disease (lethargy, excessive sloughing, reddened skin). Adults were sexed based on the presence of nuptial pads. Post-metamorphic individuals were *Bd* swabbed under their limbs and on the vascular patch, tadpoles on their mouthparts (Hyatt et al. 2007; see Supplementary methods for details). Swabs were air dried and stored dry or in 80% ethanol, with 30 paired dry- and ethanol-stored swabs collected to compare their DNA preservation efficacy. Swabs were transported in a room-temperature cooler to the University of California, Berkeley for -80˚C storage.

To characterize thermal environments experienced by *Bd* and amphibians, temperature data loggers ("iButtons"; see Supplementary methods for details) were deployed in 2018 to measure temperature every four hours. Paired iButtons were placed in aquatic and terrestrial microhabitats at 20 sites from 4,134—5,302 m asl (Figure S 1). Aquatic iButtons were placed where *P. marmoratum* tadpoles were clustering at the bottom of ponds, rather than at a standardized depth. Terrestrial iButtons were covered with rocks in locations where adult *P. marmoratum* occurred. Temperature data was downloaded from recovered iButtons in 2019.

2. *Bd* quantification and sequencing

We extracted DNA from swabs with PrepMan Ultra reagent and quantified *Bd* zoospore load using real-time polymerase chain reactions (rtPCR or qPCR; Boyle *et al.* 2004; Hyatt *et al.* 2007; see Supplementary methods for details). We determined *Bd* zoospore equivalents (ZE) by comparing sample C_t values relative to a standard curve, averaging across triplicates, and multiplying by 100 to account for dilutions during extraction and qPCR. 96 extracts were then sequenced at 240 genomic regions in an assay designed to discriminate between major *Bd* clades and maximize resolution within *Bd*GPL (Global Panzootic Lineage; Byrne *et al.* 2017; see Supplementary methods for details). We demultiplexed Illumina reads, trimmed them of primer sequences, merged read pairs with FLASH2 (Magoč & Salzberg 2011), and aligned merged reads to a reference sequence using the BWA-MEM algorithm (Li 2013; v0.7.17-r1188).

3. Phylogenetic and structure analyses of *Bd*

To process Vilcanota alignment files (BAMs), we filtered amplicons by their normalized sequencing depth and removed samples with > 25% missing data (see Supplementary methods for details), retaining 96 amplicons and 25 individuals. We called genotype likelihoods in ANGSD (v. 0.941-11-g7a5e0db; Korneliussen *et al.* 2014), outputting a BCF and beagle file. The output BCF had < 4% missing sites, which were imputed using Beagle (v. 4.1; Browing, Zhou, and Browning 2018).

We also processed dataset inclusive of previously-published, globally-representative Global Panzootic Lineage (GPL) samples, as well as UM142_A (ASIA2/BRAZIL *Bd* lineage) as an outgroup (Byrne *et al.* 2019). We subset fastqs by normalized depth and missing data as previously, retaining 137 amplicons and 104 samples. For phylogenetic analyses, I used filtered fastq to generate 'ambiguity sequences', replacing polymorphisms with IUPAC ambiguity codes and retaining only the most frequent length variant per amplicon (following Byrne et al. 2017). For PCA, I instead mapped the additional *Bd*GPL samples with BWA-MEM, filtered BAMs by normalized depth and missing data as previously, then generated a beagle in ANGSD as previously.

To understand which lineages of *Bd* are circulating in the Vilcanota, we aligned each amplicon of 'ambiguity' amino acid sequences in MUSCLE (v3.32; Edgar 2004), then concatenated these multiple sequence alignments. Using concatenated multiple sequence alignment in IQtree (v.2.3.2), we selected the substitution model minimizing the Bayesian information criterion using ModelFinder (Kalyaanamoorthy *et al.* 2017). We estimated a maximum likelihood tree for the data using the selected model (TPM2u+F+I+R2), 1000 bootstrap replicates (Hoang *et al.* 2018), and a maximum of 20000 iterations to stop.

To examine the genetic structure of Vilcanota *Bd* relative to globally-sampled *Bd*GPL, the beagle file for Vilcanota *Bd* and *Bd*GPLsequences was used to compute a covariance matrix with PCAngsd (Meisner and Albrechtsen 2018), which was subject to eigen decomposition and visualized in R (v4.0.2). To examine the local structure of Vilcanota *Bd*, we similarly computed, eigen decomposed, and visualized a PCAngsd covariance matrix of the beagle file for Vilcanota *Bd.* Finally, we tested for structure at the scale of sampling sites and of watersheds using AMOVA. AMOVA was implemented in poppr (v.2.9.6; Kamvar *et al.* 2014) using the pegas method and nearest neighbor algorithm, a missing data cutoff of 0.25, clone correction, and 1000 permutations.

4. Analysis of infection intensity and putative sublethal impacts of infection across elevations

Modelling of infection intensity and putative sublethal impacts of infection across elevations was performed in R (v4.0.2; see Supplementary methods for details). We first compared zoospore equivalents (ZE) derived from paired dry- and ethanol-stored swabs with a Wilcoxon signed-rank test, finding no significant difference in their efficacy for preserving genomic DNA ($n_{ethanol}$=30, n_{dry}=30, p-value=0.47). Frogs were considered *Bd*-positive when their swab had >1 *Bd* ZE and showed *Bd* DNA amplification for ≥2/3 triplicate qPCR reactions. Frogs were considered *Bd*-negative if no qPCR reactions amplified and zero ZE were calculated per swab. The *Bd*-status of remaining frogs was considered ambiguous.

We explored whether elevation was a good predictor of swab zoospore equivalents (ZE) using data from all *Bd*-positive individuals. We used the Spearman rank correlation test, as we expect that the relationship between elevation and swab ZE will be monotonic but not necessarily linear. An approximation of the Spearman's rank correlation p-value computation was required because some elevations were tied across the dataset.

We explored how the body condition (scaled mass index, SMI) and body size (snout vent length, SVL) of frogs responded to their elevation and *Bd* infection status, working with adults only to avoid the potentially confounding influences of developmental state (see Supplementary methods for details). Body condition can be used to evaluate the nutritional status of an amphibian in the recent past (Brodeur *et al.* 2020; Maccracken & Stebbings 2023), whereas body size can lend insight into the speed at which an amphibian developed and its nutritional status across that period (Hector *et al.* 2012; Martins *et al.* 2013; Metcalfe & Monaghan 2001; Thompson *et al.* 2021). Individuals dedicating energy to mounting an immune response or whose foraging ability has been compromised by disease may, therefore, exhibit a lower body size or condition (Warne *et al.* 2011). We calculated SMI as per Peig & Green, 2009, such that SMI was independent of SVL (Brodeur *et al.* 2020). We built a suite of linear regression models, exploring the null model and all possible combinations of elevation, infection status, and their interaction, and selected the model that minimized the Akaike Information Criterion (AIC). We tested whether the selected model met the assumptions of linear regression, and examined coefficient estimates, r^2 values, and *p*-values to interpret model importance. We explored including sex in these models, but sex data was incomplete and not perfectly reliable given the difficulty in observing nuptial pads in smaller-bodied adults. In exploratory model building, sex was consistently insignificant with a near-zero coefficient, so was excluded from final model building and selection.

RESULTS

1. Amphibian occupancy and thermal conditions along the deglaciated mountain pass

We encountered *Pleurodema marmoratum* at regular intervals across the entirety of Osjollo Pass (Figure 1a), including across the region that was glaciated only a few decades ago (Figure 1c). This continuous distribution has established a new route for contact between frogs in the Alto Urubamba and Yavero watersheds. Within their complete distribution, *P. marmoratum* are uniquely exposed to elevations from 5,200-5,400 in the Osjollo Pass habitats that have deglaciated over the past 150 years.

As predicted, iButtons revealed that increasing elevations in the Vilcanota were associated with more extreme thermal conditions in aquatic and terrestrial *P. marmoratum* microhabitats. Higher elevations were characterized by lower average daily temperatures and larger diel fluctuations in temperature (Figure 2a).

2. Genetic structure and phylogenetic placement

Vilcanota *Bd* is geographically unstructured, with samples failing to cluster in a PCA (Figure 3a) and watersheds or sites not differentiated according to AMOVA ($p>0.05$, Table S 1). This lack of structure occurs despite Vilcanota *Bd* containing many low-frequency variants after stringent filtering (87.9% variants have an allele frequency of ≤2%).

As expected, *Bd* samples from *P. marmoratum* ($n=25$) nest within the *Bd*GPL lineage. Specifically, Vilcanota *Bd* belongs to the *Bd*GPL-2 clade. Although most Vilcanota *Bd* samples nest tightly within *Bd*GPL-2 along the first and second principal components of genetic diversity in *Bd*GPL(Figure 3b), a maximum likelihood tree of *Bd*GPL samples suggests Vilcanota samples

may represent multiple strains within *Bd*GPL-2 (Figure 4). However, the maximum likelihood tree we generated from this amplicon sequencing dataset largely struggles to resolve clades within *Bd*GPL.

3. Infection intensity across elevations

Overall, about a quarter of postmetamorphic individuals were *Bd*-positive, with a small number exhibiting infection intensities consistent with chytridiomycosis in other species studied (>10k ZE; Kinney et al., 2011; Vredenburg et al. 2010) and some evidence pointing to ongoing chytridiomycosis-associated mortalities. Of 350 adults sampled, 80 (23%) were *Bd*-positive, 184 (53%) were *Bd*-negative, and the remaining 86 (25%) were not classed (<2/3 of qPCR reactions amplified or the computed infection intensity was <1 ZE). Of 83 juveniles sampled, 27 (33%) were *Bd*-positive, 45 (54%) were *Bd*-negative, and the remaining 11 (13%) were not classed. Of 232 tadpoles sampled, 229 (98.7%) were *Bd*-negative and the remaining three (1%) were not classed. Infection intensities were generally low but exhibited a broad range of values (*median*=60.28 ZE; *min*=2.3 ZE; *max*=205,360 ZE). 13 postmetamorphic individuals had infection intensities of >10,000. We found two *P. marmoratum* dead, both of which had high infection intensities: one was a juvenile with 9,705 ZE and one was an adult with 57,263 ZE. The only individual we found that we recorded as bleeding from the ventral region and appearing to be malnourished also had a high infection intensity of 19,143 ZE. We noted other individuals that were sloughing or appeared to have a pinkish, potentially irritated hue to their ventral region, but these features had no clear relationship to infection intensity.

We found support for a moderate negative relationship between elevation and individual infection intensity in *P. marmoratum*. Spearman's rank correlation test yielded a significant negative correlation correlation coefficient (ρ=-0.23; *p*-value=0.02; *n*=107). Plotting this data highlights that the maximal infection intensity of sampled frogs declines consistently with increasing elevation (Figure 5a).

4. Apparent sublethal impacts of infection across elevations

Both body condition (SMI) and body size (SVL) appeared to respond to the infection status of a frog and the interaction of infection status with elevation (Figure 5). Overall, SMI ranged from 1.27 to 4.08, with a mean value of 2.30. The model of SMI minimizing the AIC suggested that uninfected *P. marmoratum* adults decline in SMI with increasing elevation (b_{st-}=-3.14·10^{-4}; *p*-value=2.97·10^{-3}; *n*=264; Table S 2). For infected frogs, there is no longer a relationship between elevation and SMI (b_{st+}=-3.89·10^{-6}; *p*-value=0.98; *n*=264), with the mean SMI of infected frogs across elevations approximating that of uninfected frogs at extreme high elevations (mean SMI of *Bd*-positive frogs = 2.25; Figure 5b). Meanwhile, SVL ranged from 16.4 to 40.2 mm, with a mean value of 28.05 mm. The SVL model minimizing the AIC suggested that uninfected *P. marmoratum* adults increase in SVL with increasing elevation (b_{st-} = 3.25·10^{-3}; *p*-value = 1.43·10^{-3}; *n*=264). Once again, for infected frogs, the there is no longer a relationship between elevation and SVL (b_{st+} = -3.91·10^{-4}; *p*-value = 0.08; *n*=264; Table S 3), with the mean SVL of infected frogs across elevations approximating that of uninfected frogs at low elevations (mean SVL of *Bd*-positive frogs = 27.00; Figure 5c). SMI and SVL data was noisy, such that these best-supported models explain 3% of the variance in SMI and 5% of the variance in SVL.

DISCUSSION

Here, we explored how *Batrachochytrium dendrobatidis* (*Bd*) infections in Marbled four-eyed frogs (*Pleurodema marmoratum*) may have been impacted by their elevational range expansion (Seimon *et al.* 2007), combining data on amphibian occupancy, infection intensity, body size, and condition; microhabitat temperatures; and *Bd* sequencing. We documented a new route where *Bd* may be directly transmitted between populations in a recently-deglaciated mountain pass, and showed how the new elevations colonized have exposed this host-pathogen system to new thermal regimes. We found that *Bd* continues to disperse extensively at the highest elevations reached by any global amphibian, though infection intensities were somewhat constrained with increasing elevation. Finally, we found evidence that the sublethal costs of *Bd* might vary with elevation: infected frogs had more depressed body conditions at low elevations, though infected frogs at high elevations did not reach the larger body sizes achieved by their uninfected counterparts. Altogether, this study provides preliminary insights into how the climate-driven range shifts of hosts may influence EID events.

High-quality Vilcanota *Bd* sequences were *Bd*GPL-2

Whether global *Bd* epizootics were provoked by a novel or endemic pathogen remains an open question (Rosenblum *et al.* 2013). *Bd* was often present in global regions long before outbreaks were documented (Basanta *et al.* 2021; De León *et al.* 2019). Indeed, the earliest known *Bd* was swabbed from a Titicaca water frog (*Telmatobius culeus*) collected 300 km southeast of the Cordillera Vilcanota in 1863 (Burrowes & De la Riva 2017a). The various detections of *Bd* that predate epizootic events are often hypothesized to represent local *Bd* strains, with regional *Bd*-associated declines instead being attributed to the introduction of a novel lineage (Becker *et al.* 2016; Burrowes & De la Riva 2017a). The novel lineage typically indicated is the Global Panzootic Lineage (*Bd*GPL), the lineage most frequently associated with disease outbreaks, which shows genetic hallmarks of having undergone a recent spatial and demographic expansion (James *et al.* 2015; O'Hanlon *et al.* 2018; Rosenblum *et al.* 2013; Schloegel *et al.* 2012).

As we hypothesized, we identified Vilcanota *Bd* as belonging to the *Bd*GPL (Figure 3b, Figure 4), consistent with previous studies genotyping South American *Bd* west of the Brazilian Atlantic Forest (Alvarado-Rybak *et al.* 2021; Byrne *et al.* 2019; O'Hanlon *et al.* 2018; Russell *et al.* 2019). Specifically, Vilcanota *Bd* was all *Bd*GPL-2, the more derived and globalized of two major *Bd*GPL clades (James *et al.* 2015). Our sample size was limited, as only 25 Vilcanota *Bd* samples had sufficiently low levels of missing data to be included in phylogenetic and structure analyses. Further, it is worth noting that *Bd*GPL can outcompete other strains during coinfections. Therefore, it is both possible that *Bd*GPL could have ecologically displaced any *Bd* strains already circulating in the Vilcanota upon its arrival (Farrer *et al.* 2011; Jenkinson *et al.* 2018), or else that, by generally selecting swabs with higher zoospore equivalents for sequencing, we biased detection against less-virulent strains (Byrne *et al.* 2017; Farrer *et al.* 2011).

Harsh conditions do not hamper the extensive dispersal of *Bd*GPL-2 in the Vilcanota

We had hypothesized that Vilcanota *Bd* would be spatially structured because *Bd* has previously been identified as being spatially structured in the Sierra Nevada mountains of California (Rothstein *et al.* 2021). A reason proposed for the spatial structure of Sierra Nevada *Bd* is that amphibians in this region have limited activity periods due to extreme cold and occupy disjunct wetland habitats separated by high elevation peaks (Rothstein *et al.* 2021), system characteristics held in parallel with *P. marmoratum* in the Vilcanota. However, we found Vilcanota *Bd*GPL to be spatially unstructured, despite possessing abundant, low-frequency genetic variation that should allow us to detect genetic structure if present.

*Bd*GPL has almost uniformly been found to be unstructured in previous studies on local to continental scales (Alvarado-Rybak *et al.* 2021; Basanta *et al.* 2021; Byrne *et al.* 2019; Rothstein *et al.* 2021; Velo-Antón *et al.* 2012). The lack of structure in *Bd*GPL has often been interpreted as evidence for its high rates of dispersal and for its recent introduction to sampled areas, though conceivably could indicate high rates of dispersal alone. Similarly, our data is consistent with high local dispersal. However, our amplicon sequencing dataset cannot conclusively discriminate between three possible introduction scenarios: that the extensive genetic variation we observe in Vilcanota *Bd*GPL-2 was circulating in the Vilcanota before local epizootics of the early 2000s, that *Bd*GPL-2 housed substantial standing genetic variation upon an initial introduction coincident with documented regional epizootic events (Burrowes *et al.* 2020; Catenazzi *et al.* 2011; Seimon et al. 2007), or that *Bd*GPL-2 was introduced to the Vilcanota multiple times. Finding that Vilcanota *Bd*GPL-2 appears to sort into multiple clades with *Bd*GPL-2 sampled from various global locations (Figure 4; Figure S2) is more suggestive of *Bd* having been introduced to and/or exported from the Vilcanota on multiple occasions, but our phylogeny is ultimately not well-resolved.

Although we found that the elevational range shift of *P. marmoratum* created a novel opportunity for direct *Bd* tranmission between frogs across the mountain barrier of the Vilcanota, we do not necessarily conclude that this opportunity has made an important contribution to overall *Bd* dispersal on the study landscape. Previous surveys of amphibians in the Vilcanota were limited to the sourthern portion of Osjollo Pass (Seimon *et al.* 2005; Seimon *et al.* 2007; Seimon *et al.* 2017). With our field surveys, we were able to establish that *P. marmoratum* populations from the Alto Urubamba and Yavero watersheds now have new contact in Osjollo Pass (Figure 1a). However, if this new point of contact had made an important contribution to overall *Bd* dispersal, we might expect to see some evidence that genetic structure increases with distance from Osjollo Pass. Instead, we see no evidence for any isolation-by-distance in this dataset (Figure 3a). Various direct and indirect mechanisms have likely facilitated extensive and frequent *Bd* transmission across the landscape, including the amphibian trade (Catenazzi *et al.* 2010), aquaculture (Martín-Torrijos *et al.* 2016; Ortega & Hidalgo, 2008), the movements of Andean waterbirds (Burrowes & De la Riva, 2017b), or even precipitation (Kolby *et al.* 2015).

Elevation may mediate infection outcomes for these range shifting amphibians

Early studies generally found that *Bd* prevalence increased with elevation and that epizootics impacted highland sites more severely, but did not sample above 2,500 m asl in elevation (Brem & Lips, 2008; Berger *et al.* 2004; Lips 1999). These relationships are consistent with the preference of *Bd* for cool temperatures (Piotrowski *et al.* 2004; Woodhams *et al.* 2008) and the

impaired function of amphibian immune systems and skin microbiomes at colder, more thermally variable high elevations (Daskin *et al.* 2014; Jackson & Tinsley 2002). However, early *in vitro* work on *Bd* cultures demonstrating that suboptimal temperatures may slow *Bd* replication (Piotrowski *et al.* 2004; Woodhams *et al.* 2008) led to a hypothesis that *Bd* pathogenicity would be restricted to below 4,000 m asl (Pounds *et al.* 2006; Ron 2005). Indeed, subsequent studies of *Bd* dynamics between 1,000 and 4,000 m asl reported declining *Bd* prevalence or occupancy with increasing elevation (Catenazzi *et al.* 2011; Muths *et al.* 2008), perhaps due as much to increasing aridity as to cold (De la Riva & Burrowes 2011). The idea that *Bd* pathogenicity had an upper elevational limit was later undermined by severe infections documented above 4,000 m asl in the Vilcanota (Seimon *et al.* 2007; Seimon *et al.* 2005).

In the present study, we observed that *Bd* infection intensities may be constrained with increasing elevations within the range we measured, from 3,900—5,400 m asl. This finding is consistent with our expectations considering our temperature logger data in light of the thermal dependence of *Bd* replication (Voyles *et al.* 2017): *Bd* likely experiences lower population growth rates at higher elevations in the Vilcanota (Figure 2b). However, we must consider that increasing elevations also increase the exposure of *P. mamoratum* to its thermal tolerance limits in the Vilcanota, at least in terrestrial microhabitats (Figure 2b), and note that we recorded infection loads of a magnitude typically associated with chytridiomycosis (10,000 ZE; Kinney *et al.* 2011; Vredenburg *et al*. 2010) as high as 5,000 m asl (Figure 5a).

Beyond infection intensities, we assessed whether there was evidence for sublethal impacts of *Bd* infections in *P. marmoratum*, and whether these impacts might be different for frogs in the new elevations they have colonized since the end of the Little Ice Age (t,200—5,400 m asl). Work in other amphibian systems has demonstrated that *Bd* infection can impact the body size and condition of infected individuals (Burrowes *et al.* 2008; Pearl *et al.* 2009; Lowe *et al.* 2009). These impacts merit attention, since size and condition signal important information about nutritional history in amphibians; and can predict important fitness components such as fecundity, the ability to respond effectively to stress, and lifespan (Brodeur *et al.* 2020; Hector *et al.* 2012; Maccracken & Stebbings, 2023; Martins *et al.* 2013; Metcalfe & Monaghan 2001).

Body size and condition for healthy frogs along the elevational gradient had not been previously documented for *P. marmoratum*. Our best-supported models suggest that uninfected adults generally decline in body condition but increase in body size with increasing elevation. This pattern has been described in other amphibian systems, where it has sometimes been attributed to shorter activity periods due to cold weather and snowfall (Băncilă *et al.* 2010; Pope and Matthews 2002)—a mechanism that could easily apply in the Vilcanota. Higher body size with increasing elevation has also been previously described in amphibian systems. This pattern has been frequently attributed to selection for larger size at metamorphosis and/or for larger females capable of greater maternal investment (Chen *et al.* 2013; Liao *et al.* 2014; Lüddecke 2002; Räsänen *et al.* 2005; Womack & Bell 2020).

According to our data, *Bd* infection appeared to impact the relationship between elevation and both body condition and size in *P. marmoratum* adults. Regarding body condition, we found that infected adults at low elevations no longer had better condition than their high-elevation counterparts (Figure 5b). It might be tempting to attribute the apparent larger impact of infection

for lower-elevation frogs to higher *Bd* growth rates (Figure 2b) and infection intensities (Figure 5a) at lower elevations. However, body size appears to be impacted in the opposite direction: unlike uninfected frogs, infected adults at high elevations are not larger than their low-elevation counterparts (Figure 5c). The interaction of elevation and the putative sublethal costs of *Bd* infection appears to be complex, and different mechanisms may be driving the contrasting patterns we see for body size and condition.

It is important to note that associations between *Bd* status and apparent sublethal impacts to individuals are correlative in this study. We cannot know the *Bd* exposure history of sampled frogs, and do not know the direction of causality. We interpret that *Bd* is incurring sublethal impacts, but alternately *Bd* might be more likely to affect amphibian populations with lower energy reserves.

Conclusion

Climate change will continue to drive the range shifts of species across the world, so it is important that we understand their impact on host-pathogen systems, particularly in the face of increasingly common emerging infectious disease challenges. In this system, we found that the amphibian *Pleurodema marmoratum* could not escape infection by the fungal pathogen *Batrachochytrium dendrobatidis* (*Bd*) by range shifting upslope: *Bd* can infect this species and disperse readily. However, we did see some evidence that the outcome of these *Bd* infections may be impacted by the novel conditions encountered along the range expansion front, with both infection intensities and the putative sublethal impacts of infections appearing to interact with elevation. We hope this work can stimulate further questions around how host range shifts might impact pathogen dispersal and infection outcomes.

FIGURES

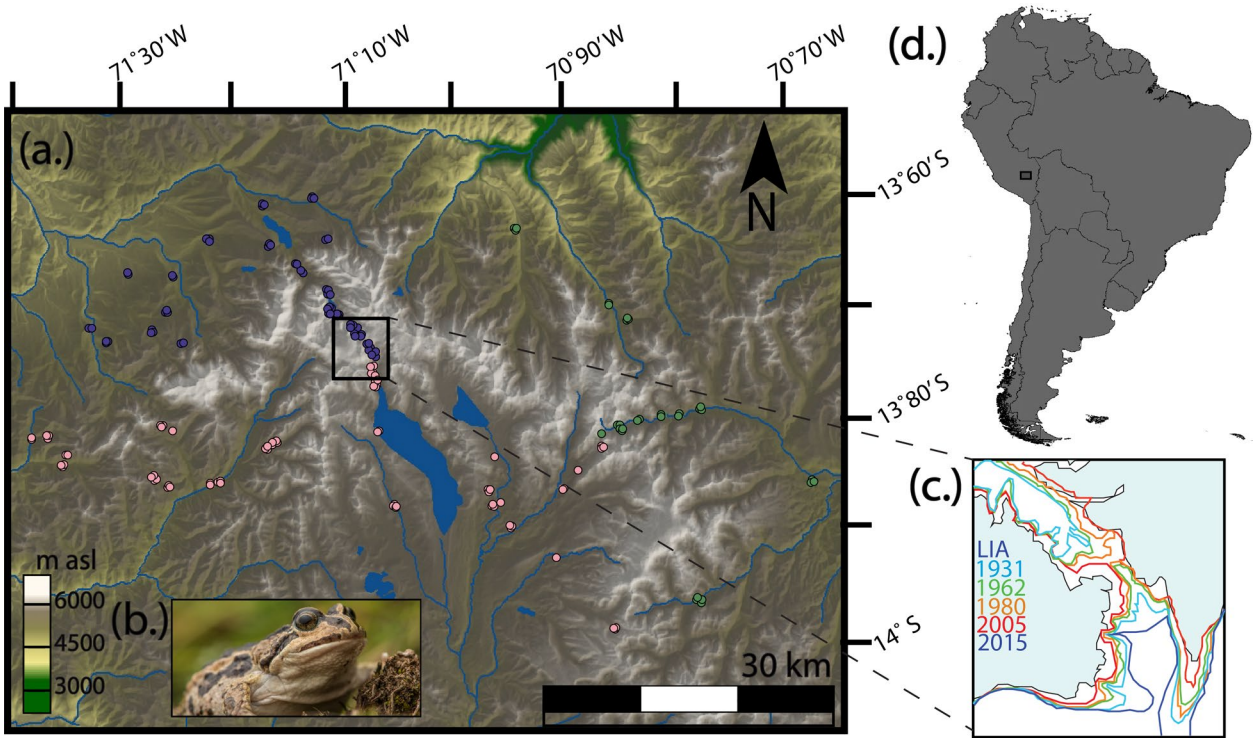

Figure 1. The study system in the Cordillera Vilcanota. (a) Sites where *Pleurodema marmormatum* were sampled for *Batrachochytrium dendrobatidis*, plotted over a hillshaded digital elevation model (DEM). Points are colored to represent their watershed assignment: the Alto Urubamba watershed is shown in pink, Inambari is shown in green, and Yavero is shown in purple. *Pleurodema marmormatum* were sampled continuously across two mountain pass transects: Osjollo Pass, the mountain pass on the western side of the landscape between Alto Urubamba and Yavero, and Chimboya Pass, the mountain pass on the eastern side between Alto Urubamba and Inambari. (b) The study species, *Pleurodema marmoratum*. Photo courtesy of Anton Sorokin. (c) Inset of Osjollo Pass showing the extent of glacial ice during the Little Ice Age (LIA) as well as in 1931, 1962, 1980, 2005, and 2015, adapter from Seimon *et al.* 2017. (d) The location of the Vilcanota within South America.

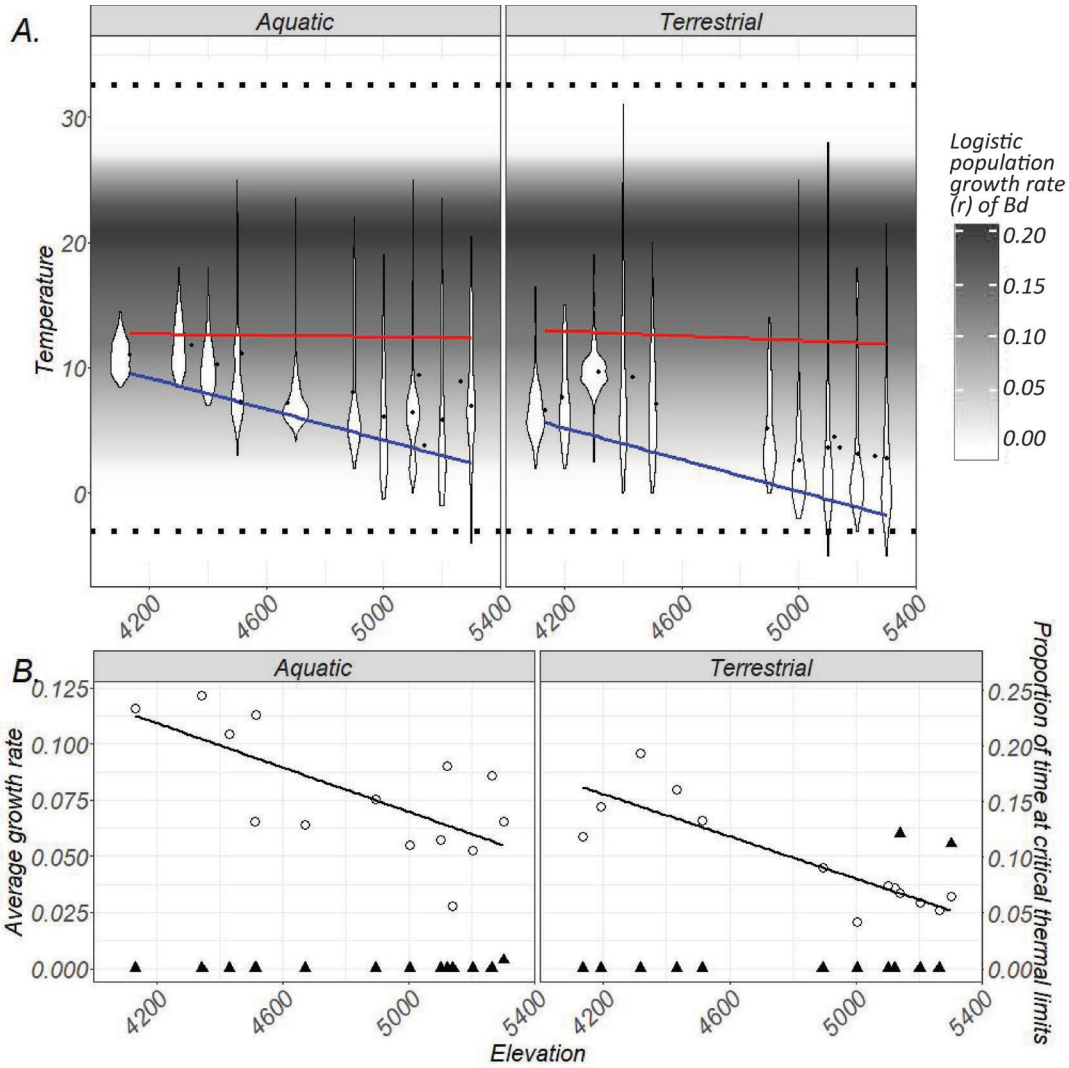

Figure 2. Thermal regimes along the elevational gradient and across microhabitats. (a) Violin plots of raw temperature data recorded by iButtons. Mean daily temperatures for each iButton are displayed as black points. The red and blue lines represent linear regression models of maximal and minimal daily temperatures, respectively. The greyscale gradient represents the logistic population growth rate (r) modelled from growth assays of a tropical *Bd* strain in culture incubated across nine different temperature treatments, ranging from 2—28˚C (from Voyles et al. 2017). The upper black dotted line represents the critical thermal maximum of adult *Pleurodema marmoratum* (32.56˚ C), and the lower dotted line represents the mean temperature tolerated by adults that recovered following freezing (-3.04˚ C; Reider et al. 2020). (b) White, unfilled points represent the average population growth rate of *Bd* according to the temperatures recorded by a given iButton, with the scale displayed on the lefthand axis. The black line represents a linear regression of this data. Black, filled triangles represent the proportion of time a given iButton was exposed to temperatures outside the physiological tolerance of adult *P. marmoratum*, with the scale displayed on the highthand axis.

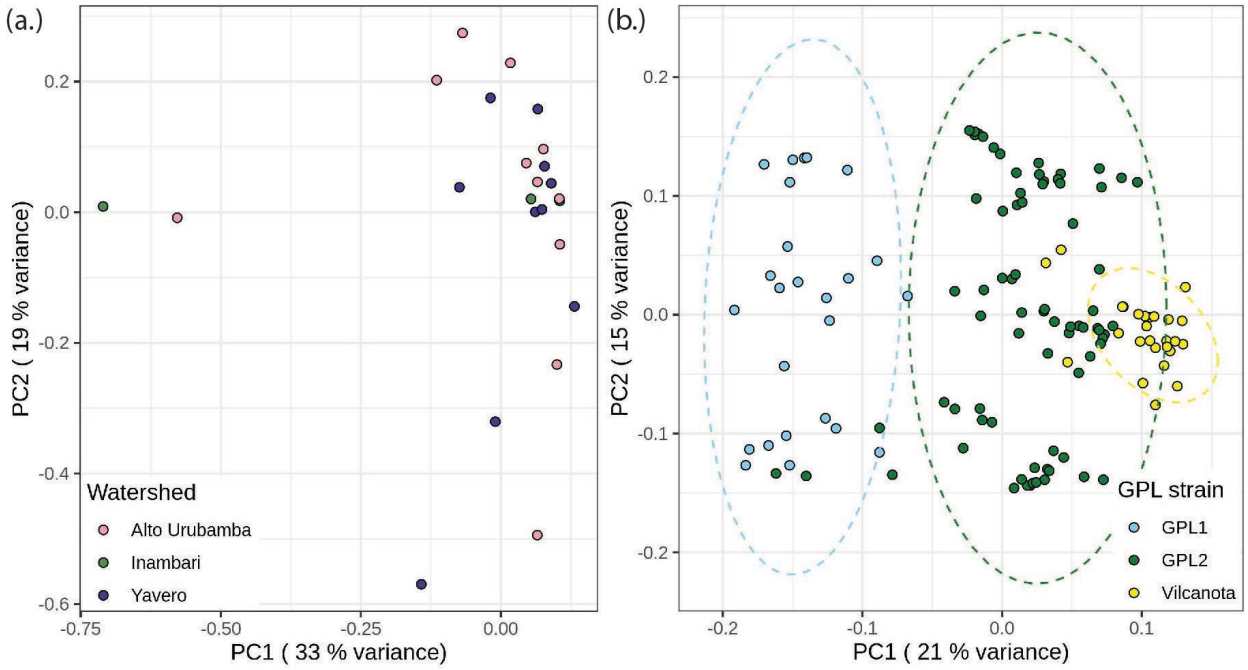

Figure 3. Principal component analyses of (a) Vilcanota samples, colored by watershed, showing their lack of spatial genetic structure, and (b) global *Bd*GPL samples, demonstrating how *Bd* sampled from the Vilcanota is nested within the *Bd*GPL-2. A version of the PCA of global *Bd*GPL samples indicating the global region of origin for each sample is shown in Figure S 2.

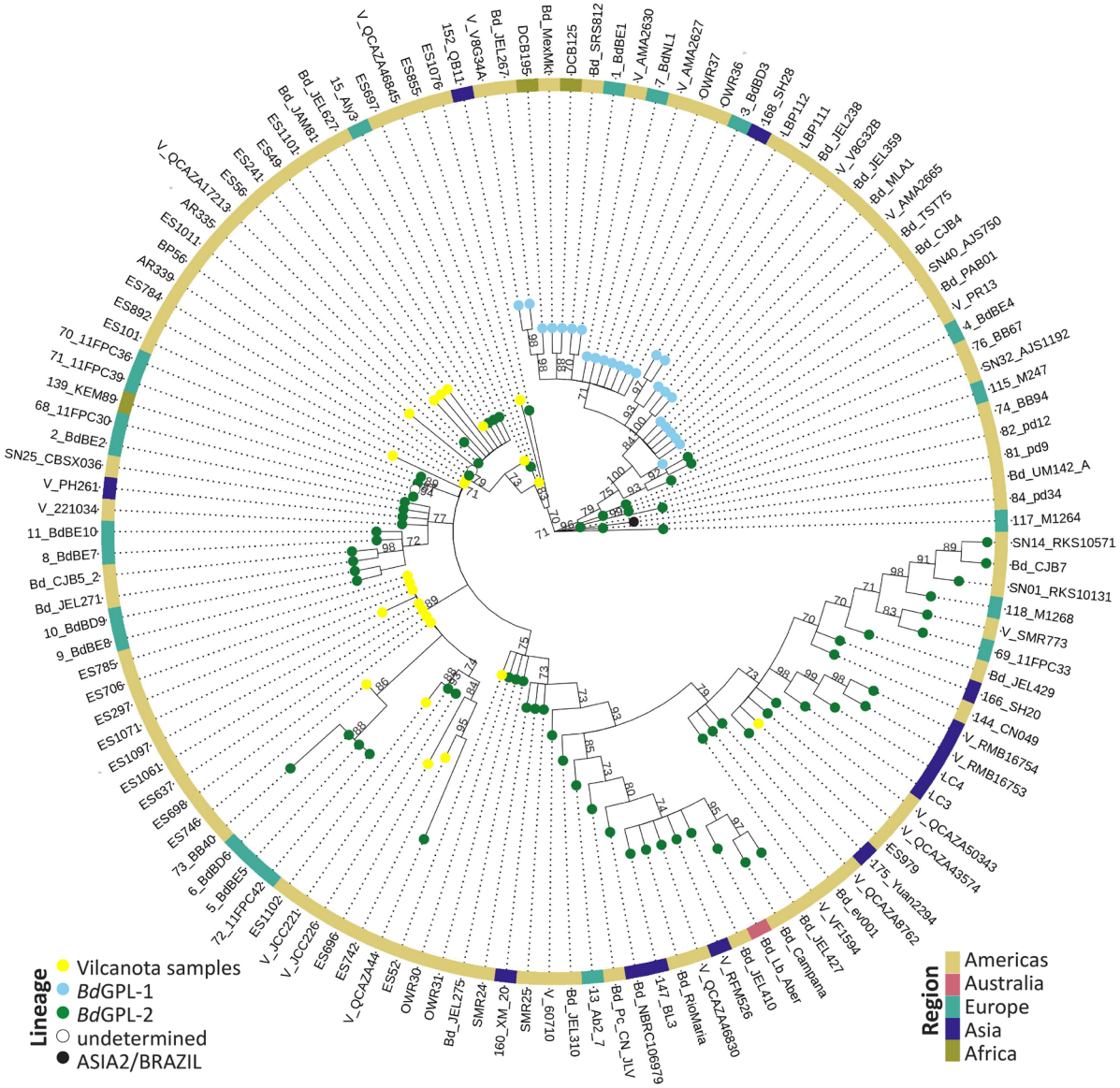

Figure 4. A maximum-likelihood tree of Vilcanota *Bd* sampled from *Pleurodema marmoratum* alongside previously-published *Bd*GPL sequences sampled globally (Byrne *et al.* 2019), rooted with a sample from the ASIA2/BRAZIL lineage of *Bd* as an outgroup. Nodes with bootstrap support values of <70 were collapsed. Assignment of *Bd*GPL samples to *Bd*GPL-1 or *Bd*GPL-2 is included whenever assigned by previous studies (James *et al.* 2015; Rothstein *et al.* 2021; Schloegel *et al.* 2012) and is shown as tip point colors. The continent of origin for samples is shown in the concentric heatmap mosaic.

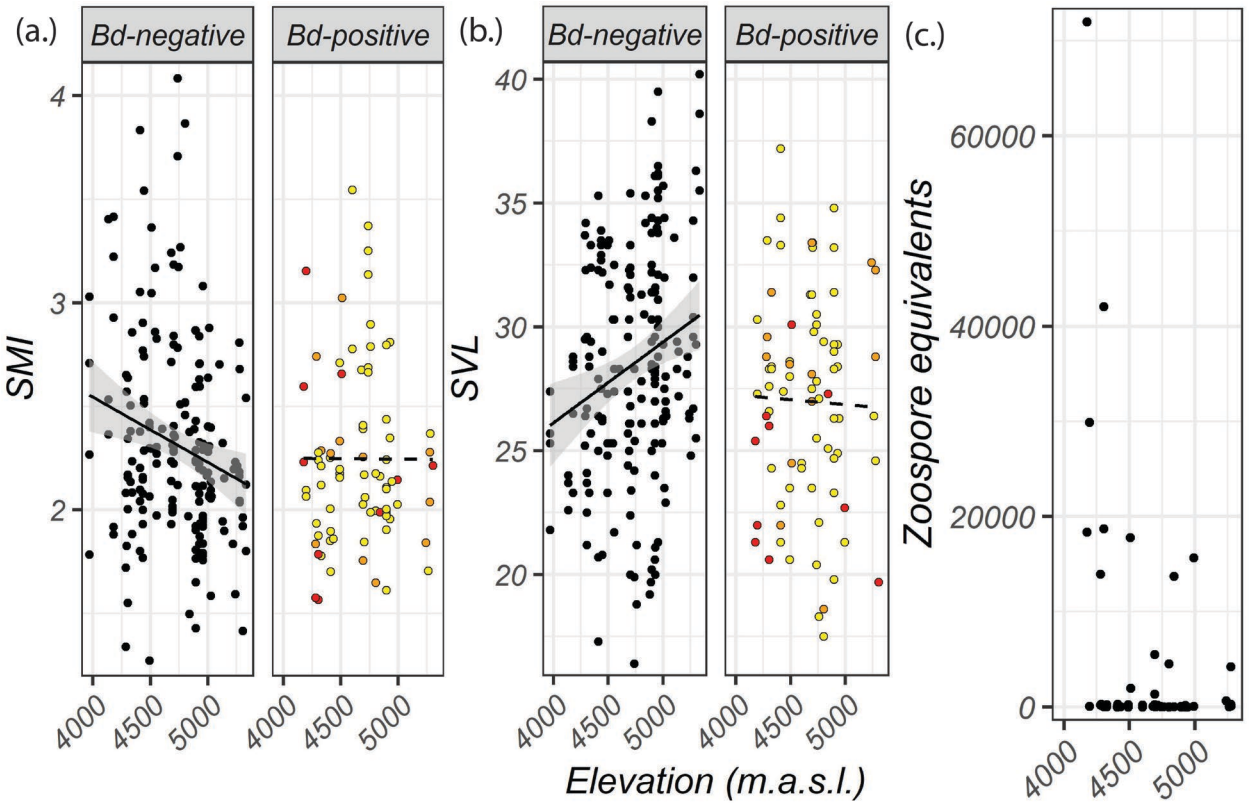

Figure 5. The relationship between elevation, putative sublethal impacts of infection, and infection intensity. (a) Zoospore equivalents for *Bd*-positive individuals across elevations sampled. (b) Body condition (scaled mass index, SMI) over elevation for *Bd*-negative and *Bd*-positive individuals. The slope of body condition over elevation at *Bd*-negative sites is significant, so a solid regression line is displayed alongside 95% confidence intervals. The slope of body condition over elevation at *Bd*-positive sites is not significant, so a dashed regression line is displayed. For *Bd*-positive individuals, those where >10,000 zoospores equivalents were quantified from their swab are shown in red, those with >200 are shown in orange, and those with >1 are shown in yellow. (c) Body size (snout-vent length, SVL) over elevation for *Bd*-negative and *Bd*-positive individuals. The slope of body size over elevation at *Bd*-negative sites is significant, so a solid regression line is displayed alongside 95% confidence intervals. The slope of body condition over elevation at *Bd*-positive sites is not significant, so a dashed regression line is displayed. *Bd*-positive individuals are colored as previously.

ACKNOWLEDGEMENTS

We are grateful to Gumercindo Crispin Condori, Jared Guevara Casafranca, Anton Sorokin, Frank Peter Condori Ccarhuarupay, Michell Frank Oruri Condori, and Isabel Diaz Huamán for critical assistance with field collection; the Crispin family for lending important items of packhorse equipment; countless families for giving kind permission to camp and graze packhorses on their land; Kelsey Reider, Tracie Seimon, and Anton Seimon for helpful conversations about planning amphibian fieldwork in the Cordillera Vilcanota; Tommy Jenkinson, Andy Rothstein, and Lydia Smith for providing advice and support on lab protocols; and to Phillip Sanvictores and Mrunali Manjrekar for excellent labwork assistance. Field and consumable lab expenses were funded by support to ECS from the Reed Scholarship from the Northern California Association of Phi Beta Kappa; the Lewis and Clark Fund for Exploration and Field Research from the American Philosophical Society; the Fellowship of Graduate Student Travel from the Society for Integrative and Comparative Biology; and the Dave and Marvalee Wake Fund from the Museum of Vertebrate Zoology, UC Berkeley. The manuscript was greatly improved thanks to comments from anonymous reviewers. ES was supported by an NSF-GRFP. This work used the Extreme Science and Engineering Discovery Environment (XSEDE), which is supported by National Science Foundation grant number ACI-1548562. Specifically, it used the Bridges-2 system, which is supported by NSF award number ACI-1928147, at the Pittsburgh Supercomputing Center (PSC). Fieldwork was conducted under research permits (Nº AUT-IFS-2018-009 and Nº AUT-IFS-2019-014) and transported under export permits (Nº 003287 and Nº 003417) granted by the Servicio Nacional Forestal y de Fauna Silvestre (SERFOR) of Peru. Importation was conducted under declaration control numbers 2018360010 and 2019672352 granted by the U.S. Fish and Wildlife Service. Animal handling was conducted according to the protocols AUP-2017-12-10585 and AUP-2018-12-11648, approved by the Animal Care and Use Committee at the University of California, Berkeley.

REFERENCES

Alvarado-Rybak, M., Acuña, P., Peñafiel-Ricaurte, A., Sewell, T. R., O'Hanlon, S. J., Fisher, M. C., Valenzuela-Sánchez, A., Cunningham, A. A., Azat, C. (2021). Chytridiomycosis outbreak in a Chilean giant frog (*Calyptocephalella gayi*) captive breeding program: genomic characterization and pathological findings. *Frontiers in Veterinary Science*, 8, 733357.

Basanta, M. D., Byrne, A. Q., Rosenblum, E. B., Piovia-Scott, J., & Parra-Olea, G. (2021). Early presence of *Batrachochytrium dendrobatidis* in Mexico with a contemporary dominance of the global panzootic lineage. *Molecular Ecology*, 30, 424–437.

Becker, C. G., Rodriguez, D., Lambertini, C., Toledo, L. F., & Haddad, C. F. B. (2016). Historical dynamics of *Batrachochytrium dendrobatidis* in Amazonia. *Ecography*, 39(10), 954–960.

Berger, L., Speare, R., Hines, H. B., Marantelli, G., Hyatt, A. D., McDonald, K. R., Skerratt, L. F., Olsen, V., Clarke, J. M., Gillespie, G., Mahony, M., Sheppard, N., Williams, C. Tyler, M. J. (2004). Effect of season and temperature on mortality in amphibians due to chytridiomycosis. *Australian Veterinary Journal*, 82(7), 31–36.

Băncilă, R. I., Hartel, T., Plăiaşu, R., Smets, J., & Cogălniceanu, D. (2010). Comparing three body condition indices in amphibians: a case study of yellow-bellied toad *Bombina variegata*. *Amphibia-Reptilia*, 31(4), 558-562.

Bosch, J., Carrascal, L. M., Durán, L., Walker, S., & Fisher, M. C. (2007). Climate change and outbreaks of amphibian chytridiomycosis in a montane area of Central Spain; is there a link? *Proceedings of the Royal Society B: Biological Sciences*, 274(1607), 253–260.

Brem, F. M. R., & Lips, K. R. (2008). *Batrachochytrium dendrobatidis* infection patterns among Panamanian amphibian species, habitats and elevations during epizootic and enzootic stages. *Diseases of Aquatic Organisms*, 81(3), 189–202.

Brodeur, J. C., Damonte, M. J., Vera Candioti, J., Poliserpi, M. B., D'Andrea, M. F., & Bahl, M. F. (2020). Frog body condition: Basic assumptions, comparison of methods and characterization of natural variability with field data from *Leptodactylus latrans*. *Ecological Indicators*, 112, 106098.

Browning, B. L., Zhou, Y., and Browning, S. R. (2018). A one-penny imputed genome from next generation reference panels. American Journal of Human Genetics 103(3):338-348.

Burrowes, P., Burrowes, P., Longo, A., Burrowes, P., & Longo, A. (2008). Potential fitness cost of *Batrachochytrium dendrobatidis* in *Eleutherodactylus coqui*, and comments on environment-related risk of infection. *Herpetotropicos*, 4(2).

Burrowes, P. A., & De la Riva, I. (2017a). Unraveling the historical prevalence of the invasive chytrid fungus in the Bolivian Andes: Implications in recent amphibian declines. *Biological Invasions*, 19, 1781–1794.

Burrowes, P., & De la Riva, I. (2017b). Detection of the amphibian chytrid fungus *Batrachochytrium dendrobatidis* in museum specimens of Andean aquatic birds: Implications for pathogen dispersal. *Journal of Wildlife Diseases*, 53(2), 349–355.

Burrowes, P. A., James, T. Y., Jenkinson, T. S., & De, I. (2020). Genetic analysis of post-epizootic amphibian chytrid strains in Bolivia: Adding a piece to the puzzle. *Transboundary and Emerging Diseases*, 67, 2163–2171.

Burrowes, P. A., Joglar, R. L., & Green, D. E. . (2004). Potential causes for amphibian declines in Puerto Rico. *Herpetologica*, 60(2), 141–154.

Bustamante, M. R., Ron, S. R., & Coloma, L. A. (2005). Cambios en la diversidad en siete comunidades de anuros en los Andes de Ecuador. *Biotropica*, 37(2), 180–189.

Byrne, A. Q., Rothstein, A. P., Poorten, T. J., Erens, J., Settles, M. L., & Rosenblum, E. B. (2017). Unlocking the story in the swab: A new genotyping assay for the amphibian chytrid fungus *Batrachochytrium dendrobatidis. Molecular Ecology Resources*, 17(6), 3218–3221.

Byrne, A. Q., Vredenburg, V. T., Martel, A., Pasmans, F., Bell, R. C., Blackburn, D. C., Bletz, M. C., Bosch, J., Briggs, C. J., Brown, R. M., Catenazzi, A., Familiar López, M., Figueroa-Valenzuela, R., Ghose, S. L., Jaeger, J. R., Jani, A. J., Jirku, M., Knapp, R. A., Muñoz, A., Portik, D. M., Richards-Zawacki, C. L., Rockney, H., Rovito, S. M., Stark, T., Sulaeman, H., Thien Tao, N., Voyles, J., Waddle, A. W., Yuan, Zhiyong Rosenblum, E. B. (2019). Cryptic diversity of a widespread global pathogen reveals expanded threats to amphibian conservation. *Proceedings of the National Academy of Sciences*, 116(41), 20382–20387.

Catenazzi, A., Lehr, E., Rodriguez, L. O., & Vredenburg, V. T. (2011). *Batrachochytrium dendrobatidis* and the collapse of anuran species richness and abundance in the Upper Manu National Park, Southeastern Peru. *Conservation Biology*, 25(2), 382–391.

Catenazzi, A., Vredenburg, V. T., & Lehr, E. (2010). *Batrachochytrium dendrobatidis* in the live frog trade of Telmatobius (Anura : Ceratophryidae) in the tropical Andes. *Diseases of Aquatic Organisms*, 92, 187–191.

Chen, W., Tang, Z. H., Fan, X. G., Wang, Y., & Pike, D. A. (2013). Maternal investment increases with altitude in a frog on the Tibetan Plateau. *Journal of Evolutionary Biology,* 26(12), 2710–2715.

Cohen, J. M., Civitello, D. J., Venesky, M. D., McMahon, T. A., Rohr, J. R. (2019). An interaction between climate change and infectious disease drove widespread amphibian declines. *Global Change Biology*, 25, 927–937.

Cohen, J. M., Venesky, M. D., Sauer, E. L., Civitello, D. J., McMahon, T. A., Roznik, E. A., & Rohr, J. R. (2017). The thermal mismatch hypothesis explains host susceptibility to an emerging infectious disease. *Ecology Letters*, 20(2), 184–193.

Daskin, J. H., Bell, S. C., Schwarzkopf, L., & Alford, R. A. (2014). Cool temperatures reduce antifungal activity of symbiotic bacteria of threatened amphibians - Implications for disease management and patterns of decline. *PLoS ONE*, 9(6), e100378.

De la Riva, I., & Burrowes, P. A. (2011). Rapid assessment of the presence of *Batrachochytrium dendrobatidis* in Bolivian Andean frogs. *Herpetological Review*, 42(3), 372–375.

De León, M. E., Zumbado-Ulate, H., García-Rodríguez, A., Alvarado, G., Sulaeman, H., Bolaños, F., & Vredenburg, V. T. (2019). *Batrachochytrium dendrobatidis* infection in amphibians predates first known epizootic in Costa Rica. *PLoS ONE*, 14(12), 1–14.

Edgar, R. C. (2004). MUSCLE: Multiple sequence alignment with high accuracy and high throughput. *Nucleic Acids Research*, 32(5), 1792–1797.

Enriquez-Urzelai, U., Bernardo, N., Moreno-Rueda, G., Montori, A., & Llorente, G. (2019). Are amphibians tracking their climatic niches in response to climate warming? A test with Iberian amphibians. *Climatic Change*, 154(1–2), 289–301.

Farrer, R. A., Weinert, L. A., Bielby, J., Garner, T. W. J., Clare, F., Bosch, J., Cunningham, Andrew A., Weldon, C., Louis, H., Anderson, L., Pond, S. L K., Shahar-Golan, R., Henka, D. A., Fisher, M. C. (2011). Multiple emergences of genetically diverse amphibian infecting chytrids include a globalized hypervirulent recombinant lineage. *PNAS*, 108(46), 1–6.

Fisher, M. C., Henk, D. A., Briggs, C. J., Brownstein, J. S., Madoff, L. C., McCraw, S. L., & Gurr, S. J. (2012). Emerging fungal threats to animal, plant and ecosystem health. *Nature*, 484(7393), 1–18.

Freeman, B. G., Scholer, M. N., Ruiz-Gutierrez, V., & Fitzpatrick, J. W. (2018). Climate change causes upslope shifts and mountaintop extirpations in a tropical bird community. *Proceedings of the National Academy of Sciences*, 115(47), 11982–11987.

Gosner, K. L. (1960). A simplified table for staging anuran embryos and larvae with notes on identification. *Herpetologica*, 16(3), 183–190.

Harvell, M. C. E., Ward, J. R., Altizer, S., Dobson, A. P., Ostfeld, R. S., & Samuel, M. D. (2002). Climate warming and disease risks for terrestrial and marine biota. *Science*, 296(5576), 2158–2162.

Hector, K. L., Bishop, P. J., & Nakagawa, S. (2012). Consequences of compensatory growth in an amphibian. *Journal of Zoology*, 286(2), 93–101.

Hoang, D.T., Chernomor, O., von Haeseler, A., Minh, B.Q., & Vinh, L.S. (2018) UFBoot2: Improving the ultrafast bootstrap approximation. *Molecular Biology and Evolution*, 35:518–522.

Hoberg, E. P., & Brooks, D. R. (2015). Evolution in action: climate change, biodiversity dynamics and emerging infectious disease. *Philosophical Transactions of the Royal Society B-Biological Sciences*, 370, 20130553.

Hyatt, A. D., Boyle, D. G., Olsen, V., Boyle, D. B., Berger, L., Obendorf, D., Dalton, A., Kriger, K., Hero, M., Hines, H., Phillott, R., Campbell, R., Marantelli, G., Gleason, F., Colling, A. (2007). Diagnostic assays and sampling protocols for the detection of *Batrachochytrium dendrobatidis. Diseases of Aquatic Organisms*, 73(3), 175–192.

Jackson, J., & Tinsley, R. (2002). Effects of environmental temperature on the susceptibility of *Xenopus laevis* and *X. wittei* (Anura) to *Protopolystoma xenopodis* (Monogenea). *Parasitology Research*, 88(7), 632–638.

Jaenson, T. G. T., & Lindgren, E. (2011). The range of *Ixodes ricinus* and the risk of contracting *Lyme borreliosis* will increase northwards when the vegetation period becomes longer. *Ticks and Tick-Borne Diseases*, 2(1), 44–49.

James, T. Y., Toledo, L. F., Rödder, D., da Silva Leite, D., Belasen, A. M., Betancourt-Román, C. M., Jenkinson, T. S., Soto-Azat, C., Lambertini, C., Longo, A. V., Ruggeri, J., Collins, J. P., Burrowes, P. A., Lips, K. R., Zamudio, Kelly R. Longcore, J. E. (2015). Disentangling host, pathogen, and environmental determinants of a recently emerged wildlife disease: Lessons from the first 15 years of amphibian chytridiomycosis research. *Ecology and Evolution*, 5(18), 4079–4097.

Jenkinson, T. S., Rodriguez, D., Clemons, R. A., Michelotti, L. A., Zamudio, K. R., Toledo, L. F., Longcore, J. E., James, T. Y., Jenkinson, T. S., James, T. Y. (2018). Globally invasive genotypes of the amphibian chytrid outcompete an enzootic lineage in coinfections. *Proceedings B*, 285, 20181894.

Jones, K. E., Patel, N. G., Levy, M. A., Storeygard, A., Balk, D., Gittleman, J. L., & Daszak, P. (2008). Global trends in emerging infectious diseases. *Nature*, 451(7181), 990–993.

Kalyaanamoorthy, S. , Minh, B.Q. , Wong, T.K.F., von Haeseler, A., & Jermiin, L.S. (2017) ModelFinder: Fast model selection for accurate phylogenetic estimates, *Nature Methods*, 14:587–589.

Kamvar, Z., Tabima, J., & Grünwald, N. (2014). Poppr: an R package for genetic analysis of populations with clonal, partially clonal, and/or sexual reproduction. *PeerJ*, 2, e281.

Kinney, V. C., Heemeyer, J. L., Pessier, A. P., & Lannoo, M. J. (2011). Seasonal pattern of *Batrachochytrium dendrobatidis* infection and mortality in *Lithobates areolatus*: Affirmation of Vredenburg's "10,000 zoospore rule." PLoS ONE, 6(3), e16708.

Kolby, J. E., Ramirez, S. D., Berger, L., Griffin, D. W., Jocque, M., & Skerratt, L. F. (2015). Presence of amphibian chytrid fungus (*Batrachochytrium dendrobatidis*) in rainwater suggests aerial dispersal is possible. *Aerobiologia*, 31(3), 411–419.

Korneliussen, T. S., Albrechtsen, A., & Nielsen, R. (2014). ANGSD : Analysis of Next Generation Sequencing Data. *BMC Bioinformatics*, 15, 356.

Lampo, M., Rodriguez-Contreras, A., La Marca, E., & Daszak, P. (2006). A chytridiomycosis epidemic and a severe dry season precede the disappearance of Atelopus species from the Venezuelan Andes. *The Herpetological Journal,* 16(4), 395–402.

Li, Y., Cohen, J. M., & Rohr, J. R. (2013). Review and synthesis of the effects of climate change on amphibians. *Integrative Zoology*, 8(2), 145–161.

Liang, L., & Gong, P. (2017). Climate change and human infectious diseases: A synthesis of research findings from global and spatio-temporal perspectives. *Environment International*, 103, 99–108.

Liao, W. B., Lu, X., & Jehle, R. (2014). Altitudinal variation in maternal investment and trade-offs between egg size and clutch size in the Andrew's toad. *Journal of Zoology*, 293(2), 84–91.

Lips, K. R. (1999). Mass mortality and population declines of anurans at an upland site in Western Panama. *Conservation Biology*, 13(1), 117–125.

Lowe, J. (2009). Amphibian chytrid (*Batrachochytrium dendrobatidis*) in post-metamorphic *Rana boylii* in inner coast ranges of central California. *Herpetological Review*, 40(2), 180–182.

Lüddecke, H. (2002). Variation and trade-off in reproductive output of the Andean frog *Hyla labialis*. *Oecologia*, 130(3), 403–410.

Maccracken, J. G., & Stebbings, J. L. (2023). Test of a body condition index with amphibians. *Journal of Herpetology*, 46(3), 346–350.

Martín-Torrijos, L., Sandoval-Sierra, J. V., Muñoz, J., Diéguez-Uribeondo, J., Bosch, J., & Guayasamin, J. M. (2016). Rainbow trout (*Oncorhynchus mykiss*) threaten Andean amphibians. *Neotropical Biodiversity*, 2(1), 26–36.

Martins, F. M. S., Oom, M. do M., Rebelo, R., & Rosa, G. M. (2013). Differential effects of dietary protein on early life-history and morphological traits in natterjack toad (*Epidalea calamita*) tadpoles reared in captivity. *Zoo Biology*, 32(4), 457–462.

Meisner, J., & Albrechtsen, A. (2018). Inferring population structure and admixture proportions in low-depth NGS data. *Genetics*, 210, 719–731.

Metcalfe, N. B., & Monaghan, P. (2001). Compensation for a bad start: Grow now, pay later? *Trends in Ecology and Evolution*, 16(5), 254–260.

Moritz, C., Patton, J. L., Conroy, C. J., Parra, J. L., White, G. C., & Beissinger, S. R. (2008). Impact of a century of climate change on small-mammal communities in Yosemite National Park, USA. *Science*, 322(5899), 261–264.

Muths, E., Pilliod, D. S., & Livo, L. J. (2008). Distribution and environmental limitations of an amphibian pathogen in the Rocky Mountains, USA. *Biological Conservation*, 141(6), 1484–1492.

O'Hanlon, S. J., Rieux, A., Farrer, R. A., Rosa, G. M., Waldman, B., Bataille, A., Kosch, T. A., Murray, K. A., Brankovics, B., Fumagalli, M., Martin, M. D., Wales, N., Alvarado-Rybak, M., Bates, K. A., Berger, L., Böll, S., Brookes, L., Frances, C. W., Wombwell, E., Zamudio, K. R., Aanensen, D. M., James, T. Y., Gilbert, M. T. P., Weldon, C., Bosch, J., Balloux, F., Garner, T. W. J., Fisher, M. C. (2018). Recent Asian origin of chytrid fungi causing global amphibian declines. *Science*, 360(6389), 621–627.

Ortega, H., & Hidalgo, M. (2008). Freshwater fishes and aquatic habitats in Peru: Current knowledge and conservation. *Aquatic Ecosystem Health and Management*, 11(3), 257–271.

Parmesan, C., Ryrholm, N., Stefanescu, C., Hill, J. K., Thomas, C. D., Descimon, H., Huntley, B., Kaila, L., Kullberg, J., Tammaru, T., Tennent, W. J., Thomas, J. A., Warren, M. (1999). Poleward shifts in geographical ranges of butterfly species associated with regional warming. *Nature*, 399, 579–583.

Pearl, C. A., Bowerman, J., Adams, M. J., & Chelgren, N. D. (2009). Widespread occurrence of the chytrid fungus *Batrachochytrium dendrobatidis* on oregon spotted frogs (*Rana pretiosa*). EcoHealth, 6(2), 209–218.

Peig, J., & Green, A. J. (2009). New perspectives for estimating body condition from mass/length data: The scaled mass index as an alternative method. *Oikos*, 118(12), 1883–1891.

Piotrowski, J. S., Annis, S. L., & Longcore, J. E. (2004). Physiology of *Batrachochytrium dendrobatidis*, a chytrid pathogen of amphibians. *Mycologia*, 96(1), 9–15.

Pope, K. L., & Matthews, K. R. (2002). Influence of anuran prey on the condition and distribution of *Rana muscosa* in the Sierra Nevada. *Herpetologica*, 58(3), 354-363.

Pounds, A. J., Bustamante, M. R., Coloma, L. A., Consuegra, J. A., Fogden, M. P. L., Foster, P. N., La Marca, E., Masters, K. L., Merino-Viteri, A., Puschendorf, R., Ron, S. R., Sánchez-Azofeifa, G. A., Still, C. J., Young, B. E. (2006). Widespread amphibian extinctions from epidemic disease driven by global warming. *Nature*, 439(7073), 161–167.

Raffel, T. R., Romansic, J. M., Halstead, N. T., McMahon, T. A., Venesky, M. D., & Rohr, J. R. (2013). Disease and thermal acclimation in a more variable and unpredictable climate. *Nature Climate Change*, 3(2), 146–151.

Räsänen, K., Laurila, A., & Merilä, J. (2005). Maternal investment in egg size: Environment- and population-specific effects on offspring performance. *Oecologia*, 142(4), 546–553.

Raxworthy, C. J., Pearson, R. G., Rabibisoa, N., Rakotondrazafy, A. M., Ramanamanjato, J. B., Raselimanana, A. P., Wu, S., Nussbaum, R. A., Stone, D. A. (2008). Extinction vulnerability of tropical montane endemism from warming and upslope displacement: A preliminary appraisal for the highest massif in Madagascar. *Global Change Biology*, 14(8), 1703–1720.

Reider, K. E., Larson, D. J., Barnes, B. M., & Donnelly, M. A. (2020). Thermal adaptations to extreme freeze–thaw cycles in the high tropical Andes. *Biotropica*, 53(1), 296–306.

Rohr, J. R., & Raffel, T. R. (2010). Linking global climate and temperature variability to widespread amphibian declines putatively caused by disease. *Proceedings of the National Academy of Sciences*, 107(18), 8269–8274.

Ron, S. R. (2005). Predicting the distribution of the amphibian pathogen *Batrachochytrium dendrobatidis* in the new world. *Biotropica*, 37(2), 209–221.

Rosenblum, E. B., James, T. Y., Zamudio, K. R., Poorten, T. J., Ilut, D., Rodriguez, D., Eastman, J. M., Richards-Hrdlicka, K., Joneson, S., Jenkinson, T. S., Longcore, J. E., Parra Olea, G., Toledo, L. F., Arellano, M. L., Medina, E. M., Restrepo, S., Flechas, S. V. Berger, L., Briggs, C. J., Stajich, J. E. (2013). Complex history of the amphibian-killing chytrid fungus revealed with genome resequencing data. *Proceedings of the National Academy of Sciences*, 110(23), 9385–9390.

Rothstein, A. P., Byrne, A. Q., Knapp, R. A., Briggs, C. J., Voyles, J., Richards-Zawacki, C. L., & Rosenblum, E. B. (2021). Divergent regional evolutionary histories of a devastating global amphibian pathogen. *Proceedings B*, 288, 20210782.

Rowe, C. L., Kinney, O. M., Fiori, A. P., & Congdon, J. D. (1996). Oral deformities in tadpoles (*Rana catesbeiana*) associated with coal ash deposition: Effects on grazing ability and growth. *Freshwater Biology*, 36, 727–730.

Russell, I. D., Larson, J. G., Von May, R., Id, I. A. H., James, Y., Davis, A. R., & Id, R. (2019). Widespread chytrid infection across frogs in the Peruvian Amazon suggests critical role for low elevation in pathogen spread and persistence. *PLoS ONE*, 14(10), e0222718.

Scheele, B. C., Pasmans, F., Skerratt, L. F., Berger, L., Martel, A., Beukema, W., Acevedo, A. A., Burrowes, P. A., Carvalho, T. (2019). Amphibian fungal panzootic causes catastrophic and ongoing loss of biodiversity. *Science*, 1463, 1459–1463.

Schloegel, L. M., Toledo, L. F., Longcore, J. E., Greenspan, S. E., Vieira, C. A., Lee, M., Zhao, S., Wangen, C., Ferreira, C. M., Hipolito, M., Davies, A. J., Cuomo, C. A., Daszak, P. J., T. Y. (2012). Novel, panzootic and hybrid genotypes of amphibian chytridiomycosis associated with the bullfrog trade. *Molecular Ecology*, 21(21), 5162–5177.

Schmidt, S. K., Nemergut, D. R., Miller, A. E., Freeman, K. R., King, A. J., & Seimon, A. (2009). Microbial activity and diversity during extreme freeze–thaw cycles in periglacial soils, 5400 m elevation, Cordillera Vilcanota. *Extremophiles*, 13, 807–816.

Seimon, T. A., Hoernig, G., Sowell, P., Halloy, S., & Seimon, A. (2005). Identification of chytridiomycosis in *Telmatobius marmoratus* at 4450 m in the Cordillera Vilcanota of southern Peru. *Monografias de Herpetologia*, 7, 273–281.

Seimon, T. A., Seimon, A., Daszak, P., Halloy, S. R. P., Schloegel, L. M., Aguilar, C. A., Sowell, P., Hyatt, A. D., Konecky, B., Simmons, J. E. (2007). Upward range extension of Andean anurans and chytridiomycosis to extreme elevations in response to tropical deglaciation. *Global Change Biology*, 13(1), 288–299.

Seimon, T. A., Seimon, A., Yager, K., Reider, K., Delgado, A., Sowell, P., Tupayachi, A., Konecky, B., McAloose, D., Halloy, S. (2017). Long-term monitoring of tropical alpine habitat change, Andean anurans, and chytrid fungus in the Cordillera Vilcanota, Peru: Results from a decade of study. *Ecology and Evolution*, 7(5), 1527–1540.

Skerratt, L. F., Berger, L., Speare, R., Cashins, S., McDonald, K. R., Phillott, A. D., Hines, Hines, H. B., Kenyon, N. (2007). Spread of chytridiomycosis has caused the rapid global decline and extinction of frogs. *EcoHealth*, 4(2), 125–134.

Thompson, C. M., & Popescu, V. D. (2021). Complex hydroperiod induced carryover responses for survival, growth, and endurance of a pond-breeding amphibian. Oecologia, 195(4), 1071-1081.

Velo-Antón, G., Rodríguez, D., Savage, A. E., Parra-olea, G., Lips, K. R., & Zamudio, K. R. (2012). Amphibian-killing fungus loses genetic diversity as it spreads across the New World. *Biological Conservation*, 146, 213–218.

Voyles, J., Johnson, L. R., Rohr, J., Kelly, R., Barron, C., Miller, D., Minster, J., Rosenblum, E. B. (2017). Diversity in growth patterns among strains of the lethal fungal pathogen *Batrachochytrium dendrobatidis* across extended thermal optima. *Oecologia*, 184(2), 363–373.

Vredenburg VT, Knapp RA, Tunstall TS, Briggs CJ (2010) Dynamics of an emerging disease drive large-scale amphibian population extinctions. *PNAS*. pnas.0914111107.

Warne, R. W., Crespi, E. J., & Brunner, J. L. (2011). Escape from the pond: Stress and developmental responses to ranavirus infection in wood frog tadpoles. *Functional Ecology*, 25(1), 139–146.

Womack, M. C., & Bell, R. C. (2020). Two-hundred million years of anuran body-size evolution in relation to geography, ecology and life history. *Journal of Evolutionary Biology*, 33(10), 1417–1432.

Woodhams, D. C., Alford, R. A., Briggs, C. J., Johnson, M., & Rollins-Smith, L. A. (2008). Life-history trade-offs influence disease in changing climates: Strategies of an amphibian pathogen. *Ecology*, 89(6), 1627–1639.

Zamora-Vilchis, I., Williams, S. E., & Johnson, C. N. (2012). Environmental temperature affects prevalence of blood parasites of birds on an elevation gradient: Implications for disease in a warming climate. *PLoS ONE*, 7(6), e39208.